

Renormalization group flow for fermionic superfluids at zero temperature

P. Strack,^{1,2,*} R. Gersch,¹ and W. Metzner¹

¹Max-Planck-Institute for Solid State Research, Heisenbergstr. 1, D-70569 Stuttgart, Germany

²Institute for Theoretical Physics, University of Heidelberg, Philosophenweg 16, D-69120 Heidelberg, Germany

(Dated: October 31, 2018)

We present a comprehensive analysis of quantum fluctuation effects in the superfluid ground state of an attractively interacting Fermi system, employing the attractive Hubbard model as a prototype. The superfluid order parameter, and fluctuations thereof, are implemented by a bosonic Hubbard-Stratonovich field, which splits into two components corresponding to longitudinal and transverse (Goldstone) fluctuations. Physical properties of the system are computed from a set of approximate flow equations obtained by truncating the exact functional renormalization group flow of the coupled fermion-boson action. The equations capture the influence of fluctuations on non-universal quantities such as the fermionic gap, as well as the universal infrared asymptotics present in every fermionic superfluid. We solve the flow equations numerically in two dimensions and compute the asymptotic behavior analytically in two and three dimensions. The fermionic gap Δ is reduced significantly compared to the mean-field gap, and the bosonic order parameter α , which is equivalent to Δ in mean-field theory, is suppressed to values below Δ by fluctuations. The fermion-boson vertex is only slightly renormalized. In the infrared regime, transverse order parameter fluctuations associated with the Goldstone mode lead to a strong renormalization of longitudinal fluctuations: the longitudinal mass and the bosonic self-interaction vanish linearly as a function of the scale in two dimensions, and logarithmically in three dimensions, in agreement with the exact behavior of an interacting Bose gas.

PACS numbers: 05.10.Cc, 67.25.D-, 71.10.Fd

I. INTRODUCTION

Interacting Fermi systems exhibit very diverse behavior on different energy scales. Composite objects and collective phenomena emerge at scales far below the bare energy scales of the microscopic degrees of freedom. This diversity of scales is a major obstacle to a numerical solution of microscopic models, since the most interesting phenomena appear only at low temperatures and in systems with very large size. It is also hard to deal with by conventional many-body methods, if one tries to treat all scales at once and within the same approximation, such as a partial resummation of Feynman diagrams.

Therefore, it seems natural to integrate degrees of freedom (bosonic and/or fermionic fields) with different energy scales successively, descending step by step from the highest scale present in the microscopic system. This generates a one-parameter family of effective actions which interpolates smoothly between the bare action of the system, as given by the microscopic Hamiltonian, and the final effective action from which all physical properties can be extracted. The vertex functions corresponding to the effective action at scale Λ obey an exact hierarchy of differential flow equations, frequently referred to as "exact" or "functional" renormalization group (fRG).¹ This hierarchy of flow equations is a transparent source of truncation schemes for a given physical problem.²

Most interacting Fermi systems undergo a phase transition associated with spontaneous symmetry breaking at low temperature. In a renormalization group flow, the instability of the normal state is signalled by a divergence of the effective two-particle interaction at a finite scale Λ_c , that is, before all degrees of freedom have been integrated out. To continue the flow below the scale Λ_c , the order parameter corresponding to the broken symmetry has to be implemented. This can be

accomplished in a purely fermionic theory or, alternatively, by introducing a bosonic order parameter field via a Hubbard-Stratonovich transformation.

In a fermionic description the order parameter can be implemented by adding an infinitesimal external symmetry breaking field to the bare Hamiltonian, which is then promoted to a finite order parameter below the scale Λ_c .³ To capture first order transitions, one has to implement the order parameter via a finite counterterm, which is added to the bare Hamiltonian and then subtracted again in the course of the flow.⁴ A relatively simple one-loop truncation⁵ of the exact fermionic flow equation hierarchy yields an exact solution of mean-field models.^{3,4,6} The same truncation with momentum-dependent vertices provides a promising approximation to treat spontaneous symmetry breaking also beyond mean-field theory. Recently it has been shown that this approximation yields quite accurate results for the fermionic gap in the ground state of the two-dimensional attractive Hubbard model for weak and moderate interactions.⁷

If the order parameter is implemented via a Hubbard-Stratonovich field, one has to deal with a coupled theory of bosons and fermions. The evolution of the effective action of this theory is again given by an exact hierarchy of flow equations for the vertex functions.^{8,9,10} A truncation of this hierarchy has been applied a few years ago to the antiferromagnetic state of the two-dimensional repulsive Hubbard model.⁸ Important features of the quantum antiferromagnet at low temperatures were captured by the flow. More recently, various aspects of superfluidity in attractively interacting Fermi systems have been studied in the fRG framework with a Hubbard-Stratonovich field for the superfluid order parameter. Approximate flow equations were discussed for the superfluid ground state,¹¹ for the Kosterlitz-Thouless transition in two-dimensional superfluids¹² and for the BCS-BEC crossover in

three-dimensional cold atomic Fermi gases.¹³

In this work we analyze the fRG flow of the *attractive* Hubbard model, using the Hubbard-Stratonovich route to symmetry breaking. The attractive Hubbard model is a prototype of a Fermi system with a superfluid low temperature phase.¹⁴ In particular, it is a popular model for the crossover from BCS-type superfluidity at weak coupling to Bose-Einstein condensation of strongly bound pairs at strong coupling.^{15,16} An experimental realization of the attractive Hubbard model is conceivable by trapping cold fermionic atoms in an optical lattice and tuning the interaction close to a Feshbach resonance.^{17,18,19}

We focus on the superfluid ground state. The importance of quantum fluctuations in the superfluid ground state has been emphasized recently in the context of the BCS-BEC crossover.²⁰ Although the long-range order is not destroyed by fluctuations in dimensions $d > 1$, the order parameter correlations are nevertheless non-trivial in $d \leq 3$. The Goldstone mode leads to severe infrared divergences in perturbation theory. A detailed analysis of the infrared behavior of fermionic superfluids has appeared earlier in the mathematical literature,²¹ where the perturbative renormalizability of the singularities associated with the Goldstone mode was established rigorously. To a large extent divergences of Feynman diagrams cancel due to Ward identities, while the remaining singularities require a renormalization group treatment. Since the fermions are gapped at low energy scales, the infrared behavior of the collective, bosonic sector in fermionic superfluids is equivalent to the one of an interacting Bose gas, where the Goldstone mode of the condensed state strongly affects the longitudinal correlations, leading to drastic deviations from mean-field theory in dimensions $d \leq 3$.^{22,23}

The purpose of our work is to construct a relatively simple truncation of the exact fRG flow which is able to describe the correct infrared asymptotic behavior, and which yields reasonable estimates for the order parameter at least for weak and moderate interaction strength. From a numerical solution of the flow equations, which we perform in two dimensions, we obtain information on the importance of Goldstone modes and other fluctuation effects.

In Sec. II we introduce the bare fermion-boson action obtained from the attractive Hubbard model by a Hubbard-Stratonovich transformation. Neglecting bosonic fluctuations, one recovers the standard mean-field theory for fermionic superfluids, as recapitulated in Sec. III. By truncating the exact fRG hierarchy, we derive approximate flow equations involving fermionic and bosonic fluctuations in Sec. IV. At the end of that section we reconsider mean-field theory from a flow equation perspective. Sec. V is dedicated to a discussion of results obtained by solving the flow equations. We discuss the asymptotic behavior in the infrared limit in two and three dimensions and then present numerical results for the flow in two dimensions, where fluctuation effects are most pronounced. Finally, we summarize our results in Sec. VI.

II. BARE ACTION

As a prototype model for the formation of a superfluid ground state in an interacting Fermi system we consider the attractive Hubbard model

$$H = \sum_{\mathbf{i}, \mathbf{j}} \sum_{\sigma} t_{\mathbf{ij}} c_{\mathbf{i}\sigma}^{\dagger} c_{\mathbf{j}\sigma} + U \sum_{\mathbf{i}} n_{\mathbf{i}\uparrow} n_{\mathbf{i}\downarrow}, \quad (1)$$

where $c_{\mathbf{i}\sigma}^{\dagger}$ and $c_{\mathbf{i}\sigma}$ are creation and annihilation operators for spin- $\frac{1}{2}$ fermions with spin orientation σ on a lattice site \mathbf{i} . For the hopping matrix we employ $t_{\mathbf{ij}} = -t$ if \mathbf{i} and \mathbf{j} are nearest neighbors on the lattice, and $t_{\mathbf{ij}} = 0$ otherwise. On a d -dimensional simple cubic lattice, this leads to a dispersion relation $\epsilon_{\mathbf{k}} = -2t \sum_{i=1}^d \cos k_i$. For the attractive Hubbard model the coupling constant U is negative.

The attractive Hubbard model has a superfluid ground state for any particle density n in $d \geq 2$ dimensions,¹⁴ provided the lattice is not completely filled ($n = 2$) or empty ($n = 0$). At half filling ($n = 1$) the usual U(1) global gauge symmetry becomes a subgroup of a larger SO(3) symmetry group, and the order parameter for superfluidity mixes with charge density order.¹⁴

Our analysis is based on a functional integral representation of the effective action, that is, the generating functional of one-particle irreducible correlation functions. For the Hubbard model, the starting point is a functional integral over fermionic fields ψ and $\bar{\psi}$ with the *bare* action

$$\Gamma_0[\psi, \bar{\psi}] = - \int_{k\sigma} \bar{\psi}_{k\sigma}(ik_0 - \xi_{\mathbf{k}}) \psi_{k\sigma} + \int_{k, k', q} U \bar{\psi}_{-k+\frac{q}{2}\downarrow} \bar{\psi}_{k+\frac{q}{2}\uparrow} \psi_{k'+\frac{q}{2}\uparrow} \psi_{-k'+\frac{q}{2}\downarrow}, \quad (2)$$

where $\xi_{\mathbf{k}} = \epsilon_{\mathbf{k}} - \mu$ is the single-particle energy relative to the chemical potential. The variables $k = (k_0, \mathbf{k})$ and $q = (q_0, \mathbf{q})$ collect Matsubara energies and momenta. We use the shorthand notation $\int_k = \int_{k_0} \int_{\mathbf{k}} = \int_{-\infty}^{\infty} \frac{dk_0}{2\pi} \int_{-\pi}^{\pi} \frac{d^d \mathbf{k}}{(2\pi)^d}$ for momentum and energy integrals, and $\int_{k\sigma}$ includes also a spin sum. We consider only *ground state* properties, such that the energy variables are continuous.

The attractive interaction drives spin-singlet pairing with s-wave symmetry and a spontaneous breaking of the global U(1) gauge symmetry. Therefore, we decouple the Hubbard interaction in the s-wave spin-singlet pairing channel by introducing a complex bosonic Hubbard-Stratonovich field ϕ_q conjugate to the bilinear composite of fermionic fields²⁴

$$\tilde{\phi}_q = U \int_k \psi_{k+\frac{q}{2}\uparrow} \psi_{-k+\frac{q}{2}\downarrow}. \quad (3)$$

This yields a functional integral over ψ , $\bar{\psi}$ and ϕ with the new bare action

$$\Gamma_0[\psi, \bar{\psi}, \phi] = - \int_{k\sigma} \bar{\psi}_{k\sigma}(ik_0 - \xi_{\mathbf{k}}) \psi_{k\sigma} - \int_q \phi_q^* \frac{1}{U} \phi_q + \int_{k, q} (\bar{\psi}_{-k+\frac{q}{2}\downarrow} \bar{\psi}_{k+\frac{q}{2}\uparrow} \phi_q + \psi_{k+\frac{q}{2}\uparrow} \psi_{-k+\frac{q}{2}\downarrow} \phi_q^*). \quad (4)$$

where ϕ^* is the complex conjugate of ϕ , while ψ and $\bar{\psi}$ are algebraically independent Grassmann variables.

Our aim is to compute fermionic and bosonic correlation functions with a focus on a correct description of the low-energy (infrared) behavior. A central object in our analysis is the *effective action* $\Gamma[\psi, \bar{\psi}, \phi]$, which can be obtained by functional integration of the bare action in the presence of source fields and a subsequent Legendre transform with respect to these fields.²⁵ Functional derivatives of $\Gamma[\psi, \bar{\psi}, \phi]$ with respect to ψ , $\bar{\psi}$, ϕ (and ϕ^*) yield the one-particle irreducible vertex functions.

III. MEAN-FIELD THEORY

As a warm-up for the renormalization group treatment it is instructive to recapitulate the mean-field theory for the superfluid phase in the functional integral formalism.²⁴ In mean-field approximation bosonic fluctuations are neglected, that is, the bosonic field ϕ is fixed instead of being integrated over all possible configurations. The fermion fields can then be integrated exactly. The (fixed) bosonic field is determined by minimizing the effective action as a functional of ϕ . For a homogeneous system, the minimizing ϕ_q can be non-zero only for $q = 0$. We denote the minimum by α . Substituting $\phi_0 \rightarrow \alpha + \phi_0$ yields

$$\begin{aligned} \Gamma_0[\psi, \bar{\psi}, \alpha + \phi] = & - \int_{k\sigma} \bar{\psi}_{k\sigma}(ik_0 - \xi_{\mathbf{k}}) \psi_{k\sigma} - \alpha^* \frac{1}{U} \alpha \\ & + \int_k (\bar{\psi}_{-k\downarrow} \bar{\psi}_{k\uparrow} \alpha + \psi_{k\uparrow} \psi_{-k\downarrow} \alpha^*) \\ & - \frac{1}{U} (\alpha^* \phi_0 + \alpha \phi_0^*) \\ & + \int_{k,q} (\bar{\psi}_{-k+\frac{q}{2}\downarrow} \bar{\psi}_{k+\frac{q}{2}\uparrow} \phi_q + \psi_{k+\frac{q}{2}\uparrow} \psi_{-k+\frac{q}{2}\downarrow} \phi_q^*) \\ & - \int_q \phi_q^* \frac{1}{U} \phi_q. \end{aligned} \quad (5)$$

A necessary condition for a minimum of the effective action is that its first derivative with respect to ϕ (or ϕ^*), that is, the bosonic 1-point function $\Gamma_b^{(1)}(q)$, vanishes. In other words, terms linear in ϕ (or ϕ^*) have to vanish in the effective action. For $q \neq 0$, $\Gamma_b^{(1)}(q)$ vanishes for any choice of α in a homogeneous system. For $q = 0$ and in mean-field approximation, the 1-point function is given by

$$\Gamma_b^{(1)}(0) = -\frac{1}{U} \alpha + \int_k \langle \psi_{k\uparrow} \psi_{-k\downarrow} \rangle \quad (6)$$

where $\langle \dots \rangle$ denotes expectation values. The first term on the right hand side corresponds to the contribution $-\frac{1}{U} \alpha \phi_0^*$ to Γ_0 in the third line of Eq. (5), while the second term is generated by contracting the fermions in the contribution proportional to ϕ_q^* in the forth line of Eq. (5). In the absence of bosonic fluctuations there is no other contribution to $\Gamma_b^{(1)}$. From the condition $\Gamma_b^{(1)}(0) = 0$ one obtains

$$\alpha = U \int_k \langle \psi_{k\uparrow} \psi_{-k\downarrow} \rangle, \quad (7)$$

which relates α to a fermionic expectation value.

We now turn to the fermionic 2-point functions. The normal fermionic propagator $G_{f\sigma}(k) = -\langle \psi_{k\sigma} \bar{\psi}_{k\sigma} \rangle$ and the anomalous propagators $F_f(k) = -\langle \psi_{k\uparrow} \psi_{-k\downarrow} \rangle$ and $\bar{F}_f(k) = -\langle \bar{\psi}_{-k\downarrow} \bar{\psi}_{k\uparrow} \rangle$ can be conveniently collected in a Nambu matrix propagator

$$\mathbf{G}_f(k) = \begin{pmatrix} G_{f\uparrow}(k) & F_f(k) \\ \bar{F}_f(k) & -G_{f\downarrow}(-k) \end{pmatrix}. \quad (8)$$

The anomalous propagators satisfy the relations $\bar{F}_f(k) = F_f^*(k)$ and $F_f(-k) = F_f(k)$. In (our) case of spin rotation invariance the normal propagator does not depend on σ , and therefore, $G_{f\uparrow}(k) = G_{f\downarrow}(k) = G_f(k)$.

In mean-field theory, the fermionic 2-point vertex function $\Gamma_f^{(2)} = -\mathbf{G}_f^{-1}$ can be read off directly from the bare action in the form Eq. (5):

$$\Gamma_f^{(2)}(k) = - \begin{pmatrix} ik_0 - \xi_{\mathbf{k}} & \alpha \\ \alpha^* & ik_0 + \xi_{-\mathbf{k}} \end{pmatrix}. \quad (9)$$

The off-diagonal elements are due to the terms in the second line of Eq. (5). Tadpole contributions which are generated from the terms in the lines 3-5 of Eq. (5) cancel exactly by virtue of the condition $\Gamma_b^{(1)} = 0$. In the absence of bosonic fluctuations there are no other contributions to $\Gamma_f^{(2)}$. Inverting $\Gamma_f^{(2)}$ and using $\xi_{-\mathbf{k}} = \xi_{\mathbf{k}}$ from reflection symmetry yields

$$G_f(k) = \frac{-ik_0 - \xi_{\mathbf{k}}}{k_0^2 + E_{\mathbf{k}}^2} \quad (10)$$

$$F_f(k) = \frac{\Delta}{k_0^2 + E_{\mathbf{k}}^2}, \quad (11)$$

where $E_{\mathbf{k}} = (\xi_{\mathbf{k}}^2 + |\Delta|^2)^{1/2}$ and $\Delta = \alpha$. We observe that in mean-field theory the bosonic order parameter α is equivalent to the gap Δ in the fermionic excitation spectrum. Eq. (6) corresponds to the BCS gap equation

$$\Delta = -U \int_k F_f(k). \quad (12)$$

We finally compute the bosonic 2-point functions in mean-field theory. The bosonic propagators $G_b(q) = -\langle \phi_q \phi_q^* \rangle$ and $F_b(q) = -\langle \phi_q \phi_{-q} \rangle = -\langle \phi_q^* \phi_q^* \rangle^*$ form the matrix propagator

$$\mathbf{G}_b(q) = \begin{pmatrix} G_b(q) & F_b(q) \\ F_b^*(q) & G_b(-q) \end{pmatrix}. \quad (13)$$

Note that $F_b(-q) = F_b(q)$. The bosonic 2-point function $\Gamma_b^{(2)}$ is equal to $-\mathbf{G}_b^{-1}$. We define a bosonic self-energy Σ_b via the Dyson equation $(\mathbf{G}_b)^{-1} = (\mathbf{G}_{b0})^{-1} - \Sigma_b$, where the bare propagator corresponding to the bare action Γ_0 is given by

$$\mathbf{G}_{b0}(q) = \begin{pmatrix} U & 0 \\ 0 & U \end{pmatrix}. \quad (14)$$

In mean-field theory, only fermionic bubble diagrams contribute to the bosonic self-energy:

$$\Sigma_b(q) = \begin{pmatrix} K(q) & L(q) \\ L^*(q) & K(-q) \end{pmatrix}, \quad (15)$$

where

$$K(q) = - \int_k G_f(k+q) G_f(-k) \quad (16)$$

$$L(q) = \int_k F_f(k+q) F_f(-k). \quad (17)$$

In the absence of bosonic fluctuations, there are no other contributions to Σ_b . Tadpole diagrams cancel due to $\Gamma_b^{(1)} = 0$. Note that $K(-q) = K^*(q)$ while $L(-q) = L(q)$. Inverting the matrix $\mathbf{G}_{b0} - \Sigma_b$ one obtains the bosonic propagator in mean-field approximation

$$\mathbf{G}_b(q) = \frac{1}{d(q)} \begin{pmatrix} U^{-1} - K(-q) & L(q) \\ L^*(q) & U^{-1} - K(q) \end{pmatrix}, \quad (18)$$

with the determinant $d(q) = |U^{-1} - K(q)|^2 - |L(q)|^2$.

Using the explicit expressions (10) and (11) for G_f and F_f , respectively, one can see that

$$U^{-1} - K(0) + |L(0)| = U^{-1} + \frac{1}{\Delta} \int_k F_f(k), \quad (19)$$

which vanishes if Δ is non-zero and satisfies the gap equation. Hence $d(q)$ has a zero and $\mathbf{G}_b(q)$ a pole in $q = 0$. This pole corresponds to the Goldstone mode associated with the spontaneous breaking of the $U(1)$ symmetry of the model. For small finite \mathbf{q} and q_0 , the leading q -dependences of $|U^{-1} - K(q)|$ and $L(q)$ are of order $|\mathbf{q}|^2$ and q_0^2 . Hence the divergence of $\mathbf{G}_b(q)$ for $q \rightarrow 0$ is quadratic in \mathbf{q} and q_0 . Continuing q_0 to real frequencies one obtains a propagating mode with a linear dispersion relation. As expected, the second pole of $d(q)$ is gapped and features a quadratic momentum dispersion.

By appropriately tailoring the fRG-truncation in Sec. IV B 2 to the results of this mean-field calculation in the superfluid phase, we incorporate the effects of transversal (Goldstone) fluctuations as well as longitudinal (radial) fluctuations into our computation.

IV. FLOW EQUATIONS

In this section we derive approximate flow equations by truncating the exact flow equation²⁶ for the effective action.

A. Exact flow equation

To simplify our notation, we use fermionic Nambu fields

$$\Psi_k = \begin{pmatrix} \psi_{k\uparrow} \\ \bar{\psi}_{-k\downarrow} \end{pmatrix}, \quad \bar{\Psi}_k = (\bar{\psi}_{k\uparrow}, \psi_{-k\downarrow}) \quad (20)$$

and bosonic Nambu fields

$$\Phi_q = \begin{pmatrix} \phi_q \\ \phi_{-q}^* \end{pmatrix}, \quad \bar{\Phi}_q = (\phi_q^*, \phi_{-q}). \quad (21)$$

The fermionic and bosonic matrix propagators are then given by $\mathbf{G}_f(k) = -\langle \Psi_k \bar{\Psi}_k \rangle$ and $\mathbf{G}_b(q) = -\langle \Phi_q \bar{\Phi}_q \rangle$, respectively. To

write down the exact flow equations it is convenient to combine fermionic and bosonic fields in a superfield \mathcal{S} , where fermions and bosons are distinguished by a statistics index $s = b, f$, that is, $\mathcal{S}_b = \Phi$ and $\mathcal{S}_f = \Psi$. The superpropagator $\mathbf{G}(q) = -\langle \mathcal{S}_q \bar{\mathcal{S}}_q \rangle$ is diagonal in the statistics index.

The flow equation describes the evolution of the effective action as a function of a flow parameter Λ , usually related to a cutoff. In this work we use sharp frequency cutoffs which exclude bosonic fields with $|\text{frequency}| < \Lambda_b$ and fermionic fields with $|\text{frequency}| < \Lambda_f$ from the functional integral. Thereby both fermionic and bosonic infrared divergences are regularized. Both cutoffs are monotonic functions of the flow parameter, $\Lambda_b(\Lambda)$ and $\Lambda_f(\Lambda)$, which vanish for $\Lambda \rightarrow 0$ and tend to infinity for $\Lambda \rightarrow \infty$. The cutoff can be implemented by adding the regulator term

$$\mathcal{R}^\Lambda = \frac{1}{2} \int_q \bar{\Phi}_q \mathbf{R}_b^\Lambda(q) \Phi_q + \int_k \bar{\Psi}_k \mathbf{R}_f^\Lambda(k) \Psi_k \quad (22)$$

to the bare action, where

$$\mathbf{R}_s^\Lambda(k) = [\mathbf{G}_{s0}(k)]^{-1} - [\chi_s^\Lambda(k_0) \mathbf{G}_{s0}(k)]^{-1} \quad (23)$$

for $s = b, f$, and $\chi_s^\Lambda(k_0) = \Theta(|k_0| - \Lambda_s)$. This term replaces the bare propagators \mathbf{G}_{s0} by $\mathbf{G}_{s0}^\Lambda = \chi_s^\Lambda \mathbf{G}_{s0}$.

Integrating $e^{-\Gamma_0 - \mathcal{R}^\Lambda}$ in the presence of source fields coupling linearly to \mathcal{S} and $\bar{\mathcal{S}}$ yields the cutoff-dependent generating functional for connected Green functions

$$G^\Lambda[\mathcal{S}', \bar{\mathcal{S}}'] = -\log \int D\mathcal{S} D\bar{\mathcal{S}} e^{-\Gamma_0[\mathcal{S}, \bar{\mathcal{S}}] - \mathcal{R}^\Lambda[\mathcal{S}, \bar{\mathcal{S}}] + (\mathcal{S}', \bar{\mathcal{S}}) + (\mathcal{S}, \bar{\mathcal{S}}')}, \quad (24)$$

where the bracket (\cdot, \cdot) is a shorthand notation for the inner product for superfields. The cutoff-dependent effective action Γ^Λ is defined as

$$\Gamma^\Lambda[\mathcal{S}, \bar{\mathcal{S}}] = \mathcal{L}G^\Lambda[\mathcal{S}, \bar{\mathcal{S}}] - \mathcal{R}^\Lambda[\mathcal{S}, \bar{\mathcal{S}}], \quad (25)$$

where $\mathcal{L}G^\Lambda$ is the Legendre transform of G^Λ . As a function of decreasing cutoff, Γ^Λ interpolates smoothly between the bare action Γ_0 for $\Lambda = \infty$ and the full effective action Γ recovered in the limit $\Lambda \rightarrow 0$.

The evolution of the effective action follows the exact flow equation

$$\frac{d}{d\Lambda} \Gamma^\Lambda[\mathcal{S}, \bar{\mathcal{S}}] = \text{Str} \frac{\mathbf{R}^\Lambda}{\Gamma^{(2)\Lambda}[\mathcal{S}, \bar{\mathcal{S}}] + \mathbf{R}^\Lambda}, \quad (26)$$

where $\mathbf{R}^\Lambda = \partial_\Lambda \mathbf{R}^\Lambda$, and

$$\Gamma^{(2)\Lambda}[\mathcal{S}, \bar{\mathcal{S}}] = \frac{\partial^2 \Gamma^\Lambda[\mathcal{S}, \bar{\mathcal{S}}]}{\partial \mathcal{S} \partial \bar{\mathcal{S}}}. \quad (27)$$

The supertrace Str traces over all indices with a plus sign for bosons and a minus sign for fermions. Note that the definitions of Γ^Λ vary slightly in the literature. In particular, Γ^Λ is frequently defined as the Legendre transform of G^Λ without subtracting the regulator term \mathcal{R}^Λ , which leads to a simple additional term in the flow equation.

To expand the functional flow equation (26) in powers of the fields, we write the Hessian of Γ^Λ as

$$\Gamma^{(2)\Lambda}[\mathcal{S}, \bar{\mathcal{S}}] = -(\mathbf{G}^\Lambda)^{-1} + \tilde{\Gamma}^{(2)\Lambda}[\mathcal{S}, \bar{\mathcal{S}}], \quad (28)$$

where $\tilde{\Gamma}^{(2)\Lambda}[\mathcal{S}, \bar{\mathcal{S}}]$ contains only terms which are at least quadratic in the fields. Defining $\mathbf{G}_R^\Lambda = [(\mathbf{G}^\Lambda)^{-1} - \mathbf{R}^\Lambda]^{-1}$ and expanding in powers of $\tilde{\Gamma}^{(2)\Lambda}$ yields

$$\begin{aligned} \frac{d}{d\Lambda} \Gamma^\Lambda &= -\text{Str}(\mathbf{R}^\Lambda \mathbf{G}_R^\Lambda) \\ &- \text{Str} \left[\mathbf{G}'_R{}^\Lambda (\tilde{\Gamma}^{(2)\Lambda} + \tilde{\Gamma}^{(2)\Lambda} \mathbf{G}_R^\Lambda \tilde{\Gamma}^{(2)\Lambda} + \dots) \right], \quad (29) \end{aligned}$$

where

$$\mathbf{G}'_R{}^\Lambda = \mathbf{G}_R^\Lambda \mathbf{R}^\Lambda \mathbf{G}_R^\Lambda. \quad (30)$$

The so-called single-scale propagator $\mathbf{G}'_R{}^\Lambda$ has support only for frequencies at the cutoffs, that is, for $|k_0| = \Lambda_s$. Expanding both sides of Eq. (29) in powers of the fields and comparing coefficients yields a hierarchy of flow equations for the vertex functions.

To describe spontaneous symmetry breaking we expand around a generally non-zero value of the $q = 0$ component of the bosonic field, that is, we expand $\Gamma^\Lambda[\psi, \bar{\psi}, \alpha^\Lambda + \phi]$ in powers of $\psi, \bar{\psi}, \phi, \phi^*$, where α^Λ may be non-zero. The expansion point α^Λ will be chosen such that the bosonic 1-point function $\Gamma_b^{(1)\Lambda}$ vanishes for all Λ . In this way tadpole contributions are avoided. The Λ -dependence of the expansion point α^Λ leads to terms proportional to $\dot{\alpha}^\Lambda = \partial_\Lambda \alpha^\Lambda$ stemming from the total Λ -derivative on the left hand side of the flow equation.

In the following we will frequently suppress the superscript Λ attached to cutoff-dependent quantities.

B. Truncation

The exact effective action contains an infinite number of terms of arbitrary order in fermionic and/or bosonic fields. We now describe which terms are kept and how they are parametrized. We keep all terms which are crucial for a qualitatively correct description of the low-energy behavior of the system. We distinguish the symmetric regime, where $\alpha = 0$, from the symmetry broken regime, where $\alpha \neq 0$. The former applies to large Λ , the latter to small Λ .

1. Symmetric regime

The bare action Eq. (4) contains quadratic terms for fermions and bosons, and an interaction term where bosons couple linearly to a fermion bilinear. In the effective action we keep these terms with generalized cutoff-dependent parameters and add a bosonic self-interaction of order $|\phi|^4$. The latter is generated by the flow and becomes crucial when the quadratic part of the bosonic potential changes sign. Other interactions generated by the flow are neglected.

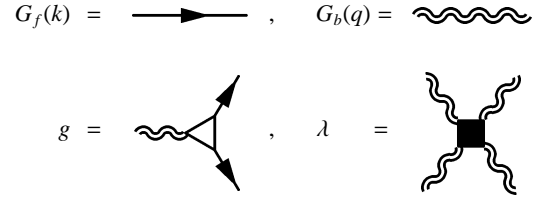


FIG. 1: Diagrammatic constituents of our truncation in the symmetric regime as described in Sec. IV B 1.

For our choice of parameters (relatively small U), the fermionic propagator receives only Fermi liquid renormalizations, leading to a slightly reduced quasi particle weight and a weakly renormalized dispersion relation. We neglect these quantitatively small effects and leave the quadratic fermionic term in the action unrenormalized, that is,

$$\Gamma_{\bar{\psi}\psi} = - \int_{k\sigma} \bar{\psi}_{k\sigma}(ik_0 - \xi_{\mathbf{k}}) \psi_{k\sigma}, \quad (31)$$

corresponding to an unrenormalized fermionic propagator

$$G_f(k) = G_{f0}(k) = \frac{1}{ik_0 - \xi_{\mathbf{k}}}. \quad (32)$$

In the bare action the term quadratic in bosons contains only a mass term. In the effective action this mass decreases with decreasing cutoff until it vanishes at a critical scale Λ_c , which marks the transition to the symmetry-broken regime. As the mass decreases, the momentum and frequency dependence of the bosonic 2-point function becomes important. The latter is generated in particular by fermionic fluctuations. For small \mathbf{q} , the leading \mathbf{q} -dependence is of order $|\mathbf{q}|^2$. The leading frequency-dependent contribution to the real part of the bosonic 2-point function is of order q_0^2 . The frequency-dependence of the imaginary part is generally of order q_0 , but the prefactor is very small, which is related to the fact that it vanishes completely in case of particle-hole symmetry. Furthermore this small imaginary part does not have any qualitative impact on the quantities we compute in the following. We therefore neglect this term and make the ansatz

$$\Gamma_{\phi^*\phi} = \frac{1}{2} \int_q \phi_q^* (m_b^2 + Z_b q_0^2 + A_b \omega_{\mathbf{q}}^2) \phi_q, \quad (33)$$

where $\omega_{\mathbf{q}}^2 = 2 \sum_{i=1}^d (1 - \cos q_i)$ is fixed, while m_b^2 , Z_b , and A_b are cutoff-dependent numbers. The function $\omega_{\mathbf{q}}^2$ has been chosen such that the quadratic momentum dependence for small \mathbf{q} is continued to a periodic function defined on the entire Brillouin zone. The initial conditions for the parameters in the bosonic 2-point function,

$$G_b(q) = - \frac{2}{Z_b q_0^2 + A_b \omega_{\mathbf{q}}^2 + m_b^2}, \quad (34)$$

can be read off from the bare action as $m_b^2 = |2/U|$ and $Z_b = A_b = 0$.

The interaction between fermions and bosons remains regular and finite near Λ_c . It can therefore be parametrized as

$$\Gamma_{\psi^2\phi^*} = g \int_{k,q} \left(\bar{\psi}_{-k+\frac{q}{2}\downarrow} \bar{\psi}_{k+\frac{q}{2}\uparrow} \phi_q + \psi_{k+\frac{q}{2}\uparrow} \psi_{-k+\frac{q}{2}\downarrow} \phi_q^* \right), \quad (35)$$

where the coupling constant g depends on the cutoff, but not on momentum and frequency. The initial condition for g is $g = 1$.

The flow generates a bosonic self-interaction which plays a crucial role near and in the symmetry-broken regime, that is, when the bosonic mass term becomes small and finally changes sign. The most relevant term is a local $|\phi|^4$ -interaction

$$\Gamma_{|\phi|^4} = \frac{\lambda}{8} \int_{q,q',p} \phi_{q+p}^* \phi_{q'-p}^* \phi_{q'} \phi_q, \quad (36)$$

where the coupling constant λ depends on the cutoff but not on momentum and frequency. The initial condition for λ is $\lambda = 0$.

The propagators and interaction vertices are represented diagrammatically in Fig. 1.

2. Symmetry broken regime

For $\Lambda < \Lambda_c$ the effective action develops a minimum at $\phi_{q=0} = \alpha \neq 0$. Due to the U(1) symmetry associated with charge conservation the minimum is degenerate with respect to the phase of α . In the following we choose α real and positive. We decompose the fluctuations of the bosonic field around α in a longitudinal (real) and a transverse (imaginary) part, σ and π , respectively:

$$\begin{aligned} \phi_q &= \sigma_q + i\pi_q \\ \phi_q^* &= \sigma_{-q} - i\pi_{-q}, \end{aligned} \quad (37)$$

where $\pi_{-q} = \pi_q^*$ and $\sigma_{-q} = \sigma_q^*$.

The bosonic part of the effective action consists of a local potential and momentum and frequency dependent contributions to the 2-point functions. A U(1)-symmetric local potential of order $|\phi|^4$ with a minimum in α has the form

$$U^{\text{loc}}[\phi] = \frac{\lambda}{8} \int (|\phi|^2 - |\alpha|^2)^2, \quad (38)$$

where ϕ is the original (unshifted) bosonic field. Substituting $\phi \rightarrow \alpha + \sigma + i\pi$ and expanding in σ and π yields a mass term for the σ -field and various interaction terms (see below). No mass term for the π -field appears, as expected, since the π -field is a Goldstone mode.²⁷

The leading momentum and frequency dependence of the bosonic 2-point function is quadratic in \mathbf{q} and q_0 , both for the σ - and π -component. Hence we make the following ansatz for the quadratic bosonic contributions to the effective action

$$\Gamma_{\sigma\sigma} = \frac{1}{2} \int_q \sigma_{-q} (m_\sigma^2 + Z_\sigma q_0^2 + A_\sigma \omega_q^2) \sigma_q \quad (39)$$

and

$$\Gamma_{\pi\pi} = \frac{1}{2} \int_q \pi_{-q} (Z_\pi q_0^2 + A_\pi \omega_q^2) \pi_q. \quad (40)$$

where m_σ , Z_σ , A_σ , Z_π , and A_π are cutoff dependent real numbers. The propagators for the σ and π fields thus have the form

$$G_\sigma(q) = -\frac{1}{m_\sigma^2 + Z_\sigma q_0^2 + A_\sigma \omega_q^2} \quad (41)$$

and

$$G_\pi(q) = -\frac{1}{Z_\pi q_0^2 + A_\pi \omega_q^2}, \quad (42)$$

respectively. The longitudinal mass is determined by the $|\phi|^4$ coupling λ and the minimum α as

$$m_\sigma^2 = \lambda |\alpha|^2. \quad (43)$$

The small imaginary contribution to $\Gamma_{\phi^*\phi}$ generated by fermionic fluctuations in the absence of particle-hole symmetry, mentioned already above, gives rise to an off-diagonal quadratic term $\Gamma_{\sigma\pi}$ with a contribution linear in q_0 . Since this term would complicate the subsequent analysis without having any significant effect, we will neglect it.

The bosonic interaction terms obtained by expanding $U^{\text{loc}}[\phi]$ are

$$\Gamma_{\sigma^4} = \gamma_{\sigma^4} \int_{q,q',p} \sigma_{-q-p} \sigma_{-q'+p} \sigma_{q'} \sigma_q, \quad (44)$$

$$\Gamma_{\pi^4} = \gamma_{\pi^4} \int_{q,q',p} \pi_{-q-p} \pi_{-q'+p} \pi_{q'} \pi_q, \quad (45)$$

$$\Gamma_{\sigma^2\pi^2} = \gamma_{\sigma^2\pi^2} \int_{q,q',p} \sigma_{-q-p} \sigma_{-q'+p} \pi_{q'} \pi_q, \quad (46)$$

$$\Gamma_{\sigma^3} = \gamma_{\sigma^3} \int_{q,q'} \sigma_{-q-q'} \sigma_{q'} \sigma_q, \quad (47)$$

$$\Gamma_{\sigma\pi^2} = \gamma_{\sigma\pi^2} \int_{q,q'} \sigma_{-q-q'} \pi_{q'} \pi_q, \quad (48)$$

with $\gamma_{\sigma^4} = \gamma_{\pi^4} = \lambda/8$, $\gamma_{\sigma^2\pi^2} = \lambda/4$, and $\gamma_{\sigma^3} = \gamma_{\sigma\pi^2} = \lambda\alpha/2$.

Let us now discuss terms involving fermions in the case of symmetry breaking. In addition to the normal quadratic fermionic term $\Gamma_{\bar{\psi}\psi}$ defined as before, see Eq. (31), the anomalous term

$$\Gamma_{\psi\psi} = \int_k (\Delta \bar{\psi}_{-k\downarrow} \bar{\psi}_{k\uparrow} + \Delta^* \psi_{k\uparrow} \psi_{-k\downarrow}) \quad (49)$$

is generated in the symmetry-broken regime, where $|\Delta|$ is a cutoff-dependent energy gap. The phase of Δ is inherited from the phase of α while its modulus is generally different, due to fluctuations. Since we have chosen α real and positive, Δ is real and positive, too. The normal and anomalous fermionic propagators G_f and F_f corresponding to $\Gamma_{\bar{\psi}\psi}$ and $\Gamma_{\psi\psi}$ have the standard mean-field form as in Eqs. (10) and (11), with $E_{\mathbf{k}} = (\xi_{\mathbf{k}}^2 + |\Delta|^2)^{1/2}$, but now Δ is not equal to α .

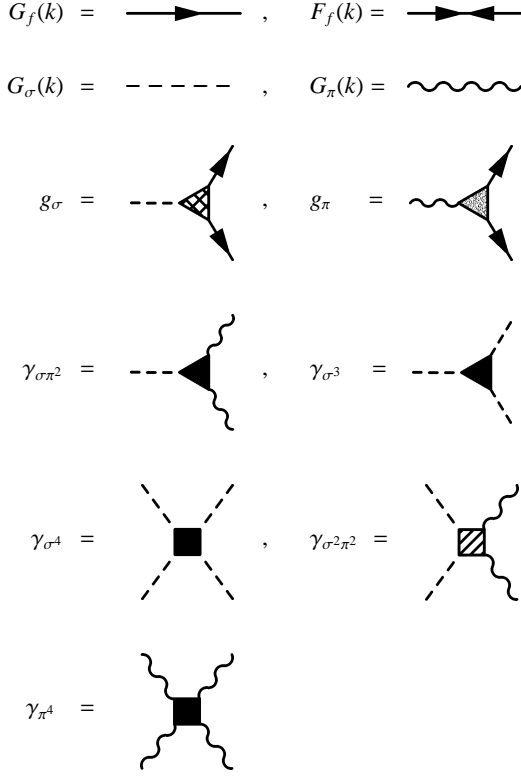


FIG. 2: Diagrammatic constituents of our truncation in the symmetry-broken regime as specified in Sec. IV B 2.

In addition to the interaction between fermions and bosons of the form Eq. (35), an anomalous term of the form

$$\Gamma_{\psi^2\phi} = \tilde{g} \int_{k,q} \left(\bar{\psi}_{-k+\frac{q}{2}\downarrow} \bar{\psi}_{k+\frac{q}{2}\uparrow} \phi_q^* + \psi_{k+\frac{q}{2}\uparrow} \psi_{-k+\frac{q}{2}\downarrow} \phi_q \right) \quad (50)$$

is generated in the symmetry-broken regime. Inserting the decomposition of ϕ in longitudinal and transverse fields into the normal and anomalous interaction terms, we obtain

$$\Gamma_{\psi^2\sigma} = g_\sigma \int_{k,q} \left(\bar{\psi}_{-k+\frac{q}{2}\downarrow} \bar{\psi}_{k+\frac{q}{2}\uparrow} \sigma_q + \psi_{k+\frac{q}{2}\uparrow} \psi_{-k+\frac{q}{2}\downarrow} \sigma_{-q} \right), \quad (51)$$

$$\Gamma_{\psi^2\pi} = ig_\pi \int_{k,q} \left(\bar{\psi}_{-k+\frac{q}{2}\downarrow} \bar{\psi}_{k+\frac{q}{2}\uparrow} \pi_q - \psi_{k+\frac{q}{2}\uparrow} \psi_{-k+\frac{q}{2}\downarrow} \pi_{-q} \right), \quad (52)$$

where $g_\sigma = g + \tilde{g}$ and $g_\pi = g - \tilde{g}$. Fermions couple with different strength to the σ - and π -field, respectively.

A diagrammatic representation of the various propagators and interaction vertices in the symmetry-broken regime is shown in Fig. 2. We finally note that in a previously reported attempt¹¹ to truncate the fRG flow in a fermionic superfluid the gap Δ was not taken into account in the fermionic propagator, and no distinction between longitudinal and transverse fields was made for the bosonic Z-factors in the symmetry-broken regime.

C. Approximate flow equations

Inserting the above ansatz for the truncated effective action into the exact flow equation and comparing coefficients yields a set of coupled flow equations for the cutoff dependent parameters. The various contributions can be conveniently represented by Feynman diagrams. The prefactors and signs in the flow equations could be extracted from the expansion of the exact flow equation, Eq. (29). However, in practice we determine them by comparison to a conventional perturbation expansion.

All contributions to our flow equations correspond to one-loop diagrams with only one momentum and frequency integration, as dictated by the structure of the exact flow equation in the form (29). One of the propagators in the loop is a bosonic or fermionic component of the single-scale propagator \mathbf{G}'_R , the others (if any) are components of \mathbf{G}_R .

For a sharp frequency cutoff the frequency variable running around the loop is pinned by $\mathbf{G}'_R(k_0)$ to $k_0 = \pm\Lambda_b$ or $k_0 = \pm\Lambda_f$. Hence the frequency integral can be performed analytically. The problem that the integrand contains also step functions $\chi_s^\Lambda(k_0) = \Theta(|k_0| - \Lambda_s)$ can be treated by using the identity $\int dx \delta(x - x_0) f[x, \Theta(x - x_0)] = \int_0^1 du f(x_0, u)$, which is valid for any smooth function f .

More specifically, in the present case the one-loop diagrams are evaluated for vanishing external frequencies, such that all internal propagators carry the same frequency. In loops involving only either only bosonic or only fermionic propagators, one can use the identity

$$n \int dk_0 \mathbf{G}'_{sR}(k_0) \mathbf{A} [\mathbf{G}_{sR}(k_0) \mathbf{A}]^{n-1} = \Lambda'_s \sum_{k_0=\pm\Lambda_s} [\mathbf{G}_s(k_0) \mathbf{A}]^n, \quad (53)$$

valid for any matrix \mathbf{A} , to replace the frequency integration by a frequency sum over $\pm\Lambda_s$ while replacing all the propagators in the loop by \mathbf{G}_s . The factor n corresponds to the n possible choices of positioning \mathbf{G}'_{sR} in a loop with n lines, and $\Lambda'_s = \partial\Lambda_s/\partial\Lambda$. For $\Lambda_b = \Lambda_f$ the above formula holds also for the superpropagator \mathbf{G}_R , such that it applies also to loops with mixed products of bosonic and fermionic propagators. For $\Lambda_b \neq \Lambda_f$, mixed loops contribute only if the single-scale propagator is associated with the larger cutoff. For example, for $\Lambda_b > \Lambda_f$, the single-scale propagator has to be bosonic, since \mathbf{G}_b vanishes at $|k_0| = \Lambda_f$. On the other hand, for $|k_0| = \Lambda_b$ one has $\mathbf{G}_{fR}(k_0) = \mathbf{G}_f(k_0)$, and for the integration of the bosonic factors in the loop one can again use Eq. (53).

For loop integrals involving the frequency sum over $\pm\Lambda_s$ and the momentum integral over the Brillouin zone we use the short-hand notation

$$\int_{k|\Lambda_s} = \frac{\Lambda'_s}{2\pi} \sum_{k_0=\pm\Lambda_s} \int \frac{d^d k}{(2\pi)^d}, \quad (54)$$

where $\Lambda'_s = \partial\Lambda_s/\partial\Lambda$.

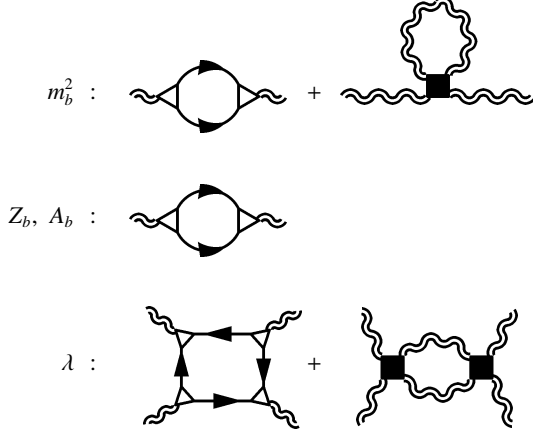


FIG. 3: Feynman diagrams representing the flow equations in the symmetric regime.

1. Symmetric regime

Here we choose $\Lambda_b = \Lambda_f = \Lambda$. One is in principle free to choose the fermionic and bosonic cutoff independently. We have checked that the concrete choice of Λ_b and Λ_f in the symmetric regime does not change the final results for $\Lambda \rightarrow 0$ much. The Feynman diagrams contributing to the flow in the symmetric regime are shown in Fig. 3.

The flow of the bosonic mass is given by the bosonic self-energy at vanishing external momentum and frequency, that is,

$$\partial_\Lambda \frac{m_b^2}{2} = g^2 \int_{k|\Lambda} G_f(k) G_f(-k) + \frac{\lambda}{2} \int_{q|\Lambda} G_b(q). \quad (55)$$

The fermionic contribution to $\partial_\Lambda m_b^2$ is positive, leading to a reduction of m_b^2 upon decreasing Λ , while the bosonic fluctuation term is negative (since $G_b(q) < 0$). The flow of Z_b is obtained from the second frequency derivative of the bosonic self-energy as

$$\partial_\Lambda Z_b = g^2 \int_{k|\Lambda} \partial_{q_0}^2 G_f(k+q) G_f(-k) \Big|_{q=0}. \quad (56)$$

Similarly, the flow of A_b is obtained from a second momentum derivative of the bosonic self-energy:

$$\partial_\Lambda A_b = g^2 \int_{k|\Lambda} \partial_{\mathbf{q}}^2 G_f(k+q) G_f(-k) \Big|_{q=0}, \quad (57)$$

where $\partial_{\mathbf{q}}^2 = \frac{1}{d} \sum_{i=1}^d \partial_{q_i}^2$. Since the bosonic self-energy is isotropic in \mathbf{q} to leading (quadratic) order in \mathbf{q} , the results do not depend much on the direction in which the momentum derivative is taken. The bosonic tadpole diagram in Fig. 3 contributes only to m_b , not to Z_b and A_b , since it yields a momentum and frequency independent contribution to the self-

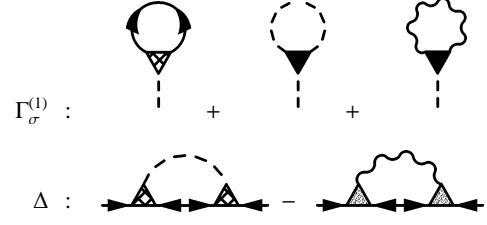


FIG. 4: Contributions to the bosonic 1-point vertex and fermion gap below Λ_c .

energy. Finally, the flow of the $|\phi|^4$ coupling is given by

$$\partial_\Lambda \lambda = -4g^4 \int_{k|\Lambda} [G_f(k)]^2 [G_f(-k)]^2 + \frac{5}{4} \lambda^2 \int_{q|\Lambda} [G_b(q)]^2. \quad (58)$$

Within the truncation of the effective action described in Sec. IV.B there is no contribution to the flow of the interaction between fermions and bosons in the symmetric phase. The coupling g remains therefore invariant.

2. Symmetry broken regime

In the limit $\Lambda \rightarrow 0$ we are forced to choose $\Lambda_f \ll \Lambda_b$ to avoid an artificial strong coupling problem, as will become clear below. We therefore choose $\Lambda_f < \Lambda_b$ in the entire symmetry broken regime, which implies that the frequencies in mixed loops with bosonic and fermionic propagators are pinned at the bosonic cutoff. The precise choice of the cutoffs will be specified later.

We first derive the flow equation for the minimum of the bosonic potential α , which is derived from the condition that the bosonic 1-point vertex $\Gamma_\sigma^{(1)}$ be zero for all Λ . The flow equation for $\Gamma_\sigma^{(1)}$ reads

$$\partial_\Lambda \Gamma_\sigma^{(1)} = m_\sigma^2 \partial_\Lambda \alpha + 2g_\sigma \int_{k|\Lambda_f} F_f(k) + \frac{\lambda\alpha}{2} \int_{q|\Lambda_b} [3G_\sigma(q) + G_\pi(q)]. \quad (59)$$

The various contributions are represented diagrammatically in Fig. 4. The first term is due to the cutoff-dependence of the expansion point around which the effective action is expanded in powers of the fields. The condition $\partial_\Lambda \Gamma_\sigma^{(1)} = 0$ yields

$$\partial_\Lambda \alpha = -\frac{2g_\sigma}{m_\sigma^2} \int_{k|\Lambda_f} F_f(k) - \frac{1}{2\alpha} \int_{q|\Lambda_b} [3G_\sigma(q) + G_\pi(q)]. \quad (60)$$

We have used Eq. (43) to simplify the last term. The fermionic contribution to $\partial_\Lambda \alpha$ is negative, leading to an increase of α upon decreasing Λ , while the bosonic fluctuation term is positive and therefore reduces α . The behavior of Eq. (60) in the vicinity of the critical scale, $\Lambda \lesssim \Lambda_c$, when α and m_σ^2 are small is shown below in Sec. V A.

The flow of Δ is obtained from the flow of the anomalous

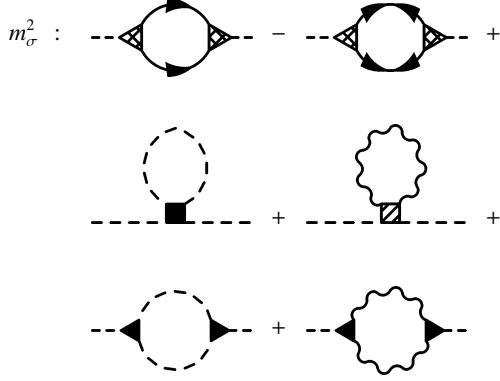


FIG. 5: Diagrammatic representation of the contributions to the bosonic mass in the symmetry-broken regime.

component of the fermionic self-energy as

$$\partial_\Lambda \Delta = g_\sigma \partial_\Lambda \alpha - \int_{q|\Lambda_b} F_f(q-k) [g_\sigma^2 G_\sigma(q) - g_\pi^2 G_\pi(q)] \Big|_{k=(0, \mathbf{k}_f)}. \quad (61)$$

The first term, due to the cutoff-dependence of the expansion point for the effective action, links the flow of the fermionic gap to the flow of the bosonic order parameter. The second term captures a correction to the relation between α and Δ due to bosonic fluctuations as illustrated in Fig. 4.

The flow of the mass of the longitudinal order parameter fluctuations (cf. Fig. 5) is obtained from the self-energy of the σ fields at zero momentum and frequency as

$$\begin{aligned} \partial_\Lambda \frac{m_\sigma^2}{2} &= g_\sigma^2 \int_{k|\Lambda_f} [G_f(k)G_f(-k) - F_f(k)F_f(-k)] + 3\frac{\lambda\alpha}{2} \partial_\Lambda \alpha \\ &+ \frac{\lambda}{4} \int_{q|\Lambda_b} [3G_\sigma(q) + G_\pi(q)] \\ &+ \frac{(\lambda\alpha)^2}{2} \int_{q|\Lambda_b} [9G_\sigma^2(q) + G_\pi^2(q)]. \end{aligned} \quad (62)$$

The second term in this equation is due to a product of the 3-point vertex γ_{σ^3} and $\partial_\Lambda \alpha$ arising from the cutoff dependence of the expansion point for the effective action. The flow of λ can be computed from the flow of m_σ^2 and α via the relation Eq. (43), $\lambda = m_\sigma^2/|\alpha|^2$.

The flow of Z_σ is obtained from the second frequency derivative of the self-energy of the σ fields, which yields

$$\begin{aligned} \partial_\Lambda Z_\sigma &= g_\sigma^2 \int_{k|\Lambda_f} \partial_{q_0}^2 [G_f(k+q)G_f(-k) - F_f(k+q)F_f(-k)] \Big|_{q=0} \\ &+ \frac{(\lambda\alpha)^2}{2} \int_{k|\Lambda_b} \partial_{q_0}^2 [9G_\sigma(k+q)G_\sigma(k) + G_\pi(k+q)G_\pi(k)] \Big|_{q=0}. \end{aligned} \quad (63)$$

The flow of A_σ is given by the same equation with $\partial_{q_0}^2$ replaced by $\partial_{\mathbf{q}}^2$.

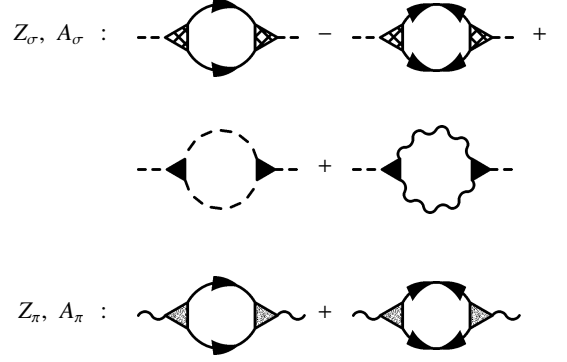


FIG. 6: Diagrams renormalizing the bosonic Z- and A-factors for $\Lambda < \Lambda_c$.

In the flow of Z_π there are strong cancellations of different terms originating from bosonic fluctuations. These cancellations are related to Ward identities which guarantee that Z_π remains finite such that the Goldstone mode is not renormalized substantially.²³ Hence, we keep only the fermionic fluctuations, that is,

$$\partial_\Lambda Z_\pi = g_\pi^2 \int_{k|\Lambda_f} \partial_{q_0}^2 [G_f(k+q)G_f(-k) + F_f(k+q)F_f(-k)] \Big|_{q=0}. \quad (64)$$

For the flow of A_π we obtain the same equation with $\partial_{q_0}^2$ replaced by $\partial_{\mathbf{q}}^2$. The terms contributing to the flow of the Z- and A-factors are illustrated diagrammatically in Fig. 6.

In the symmetry broken regime, there are also contributions to the flow of the interaction between fermions and bosons due to vertex corrections with bosonic fluctuations (see Fig. 7), yielding

$$\begin{aligned} \partial_\Lambda g_\sigma &= g_\sigma \int_{q|\Lambda_b} \left[F_f^2(k-q) - |G_f(k-q)|^2 \right] \Big|_{k=(0, \mathbf{k}_f)} \\ &\left[g_\sigma^2 G_\sigma(q) - g_\pi^2 G_\pi(q) \right], \end{aligned} \quad (65)$$

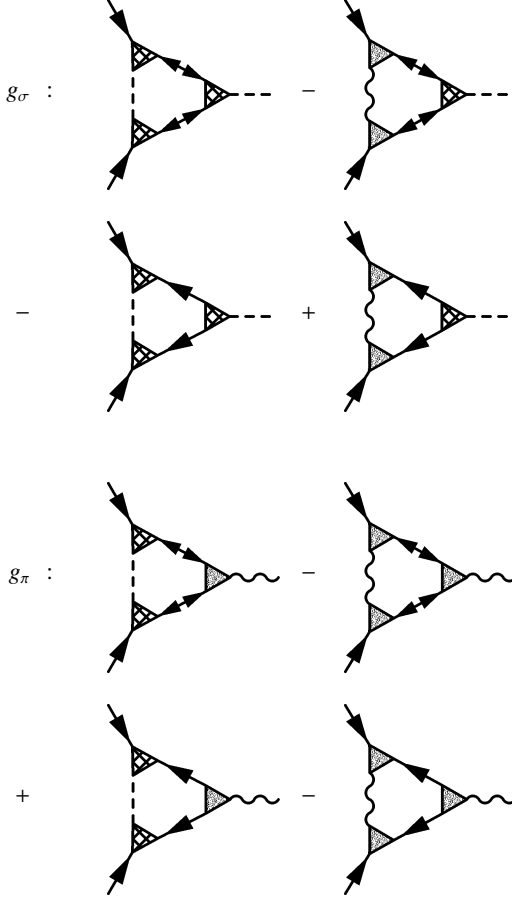
and

$$\begin{aligned} \partial_\Lambda g_\pi &= g_\pi \int_{q|\Lambda_b} \left[F_f^2(k-q) + |G_f(k-q)|^2 \right] \Big|_{k=(0, \mathbf{k}_f)} \\ &\left[g_\sigma^2 G_\sigma(q) - g_\pi^2 G_\pi(q) \right]. \end{aligned} \quad (66)$$

The right hand sides are dominated by the contribution from the π propagator, which tends to reduce g_σ, g_π for decreasing Λ .

D. Relation to mean-field theory

Before solving the flow equations derived above, we first analyze what happens when contributions due to bosonic fluctuations

FIG. 7: Fermion-boson vertex corrections below Λ_c .

tuations are neglected, and relate the reduced set of equations to the usual mean-field theory (Sec. III).

In the absence of bosonic fluctuations, $g = g_\sigma = g_\pi = 1$. Furthermore, the bosonic order parameter α and the fermionic gap Δ are identical: $\alpha = \Delta$. Since the bosonic cutoff is irrelevant here, we can choose $\Lambda_f = \Lambda$.

The flow equation for the bosonic mass in the symmetric regime, Eq. (55), simplifies to

$$\partial_\Lambda \frac{m_b^2}{2} = \int_{k|\Lambda} G_f(k) G_f(-k), \quad (67)$$

where $G_f(k) = G_{f0}(k) = (ik_0 - \xi_{\mathbf{k}})^{-1}$. This equation can be easily integrated, yielding

$$\frac{m_b^2}{2} = \frac{1}{|U|} - \int_{|k_0|>\Lambda} \int_{\mathbf{k}} \frac{1}{k_0^2 + \xi_{\mathbf{k}}^2}. \quad (68)$$

m_b vanishes at a critical scale $\Lambda_c > 0$.

The flow equation for Δ ($= \alpha$) in the symmetry broken regime $\Lambda < \Lambda_c$, Eq. (61), is reduced to

$$\partial_\Lambda \Delta = -\frac{2}{m_\sigma^2} \int_{k|\Lambda} F_f(k). \quad (69)$$

It is complemented by the flow equation for the mass of the σ field, Eq. (62), which becomes

$$\partial_\Lambda \frac{m_\sigma^2}{2} = \int_{k|\Lambda} \left[|G_f(k)|^2 - F_f^2(k) \right] + 3\gamma_{\sigma^3} \partial_\Lambda \Delta \quad (70)$$

in the absence of bosonic fluctuations, with $\gamma_{\sigma^3} = \lambda\Delta/2 = m_\sigma^2/(2\Delta)$. The propagators G_f and F_f have the usual BCS form, as in Eqs. (10) and (11).

A numerical solution of the coupled flow equations (69) and (70) yields a gap Δ which is a bit smaller than the BCS result obtained from the gap equation (12). The reason for this discrepancy is the relatively simple quartic ansatz (38) for the bosonic potential. The complete bosonic potential is non-polynomial in $|\phi|^2$ even in mean-field theory. Restricted to the zero momentum and frequency component of ϕ it has the form²⁴

$$U^{\text{MF}}(\phi) = \frac{|\phi|^2}{|U|} - \int_{\mathbf{k}} \ln \frac{k_0^2 + \xi_{\mathbf{k}}^2 + |\phi|^2}{k_0^2 + \xi_{\mathbf{k}}^2}. \quad (71)$$

The kernel of the 3-point vertex γ_{σ^3} obtained from an expansion of this mean-field potential around a finite order parameter Δ reads

$$\gamma_{\sigma^3} = -2 \int_{\mathbf{k}} \left[\frac{1}{3} F_f^3(k) - F_f(k) |G_f(k)|^2 \right] \quad (72)$$

at zero frequencies and momenta. Inserting this into (70), the flow of m_σ^2 can be written as a total derivative

$$\partial_\Lambda \frac{m_\sigma^2}{2} = -\partial_\Lambda \int_{|k_0|>\Lambda} \int_{\mathbf{k}} \left[|G_f(k)|^2 - F_f^2(k) \right], \quad (73)$$

where the Λ -derivative on the right hand side acts also on Δ , generating the term proportional to γ_{σ^3} . Integrating this equation with the initial condition $m_\sigma = 0$ at $\Lambda = \Lambda_c$, yields

$$\frac{m_\sigma^2}{2} = K(0) + L(0) - U^{-1}, \quad (74)$$

which is the correct mean-field result. With m_σ given by (74), the flow equation (69) yields the correct mean-field gap. The easiest way to see this, is to write the BCS gap equation in the presence of a cutoff in the form $1 = -U \int_{|k_0|>\Lambda} \int_{\mathbf{k}} \Delta^{-1} F_f(k)$, and take a derivative with respect to Λ .

It is instructive to relate the above flow equations for Δ and m_σ to the flow equations for the BCS mean-field model obtained in a purely fermionic RG.³ For a sharp frequency cutoff, those flow equations have the form

$$\partial_\Lambda \Delta = -(V + W) \int_{\mathbf{k}} F_f(k), \quad (75)$$

$$\partial_\Lambda (V + W) = (V + W)^2 \partial_\Lambda \int_{|k_0|>\Lambda} \int_{\mathbf{k}} \left[|G_f(k)|^2 - F_f^2(k) \right], \quad (76)$$

where V is a normal two-fermion interaction in the Cooper channel, while W is an anomalous interaction corresponding to annihilation (or creation) of four particles. With the identification $2/m_\sigma^2 = V + W$ these equations are obviously equivalent to (69) and (73). The above flow equation for $V + W$

is obtained from a one-loop truncation complemented by additional self-energy insertions drawn from higher order diagrams with tadpoles.^{3,5} These additional terms correspond to the contractions with γ_{σ^3} in the present bosonized RG.

V. RESULTS

A. Flow for $\Lambda \lesssim \Lambda_c$

For Λ slightly below Λ_c , the flow equations can be expanded in the order parameter. To leading order, the order parameter α and the gap Δ are identical, $\alpha = \Delta$. The fluctuation term in the flow equation (61) for Δ is quadratic in α , and also the flow of g_σ yields only corrections beyond linear order to the relation between α and Δ .

Near Λ_c , the flow equation (60) for α can be written as

$$\partial_\Lambda \alpha^2 = -\frac{4}{\lambda} I - \int_{q|\Lambda_b} [3G_\sigma(q) + G_\pi(q)], \quad (77)$$

where $I = \int_{k|\Lambda_f} (k_0^2 + \vec{\xi}_k^2)^{-1}$, evaluated for $\Lambda = \Lambda_c$. Note that we have replaced the ratio m_σ^2/α^2 by λ in the first term on the right hand side of the flow equation. Integrating the flow equation one obtains

$$\alpha^2 = \left[\frac{4}{\lambda} I + \int_{q|\Lambda_b} [3G_\sigma(q) + G_\pi(q)] \right]_{\Lambda=\Lambda_c} (\Lambda_c - \Lambda) \quad (78)$$

for $\Lambda \lesssim \Lambda_c$. The order parameter α and the fermionic gap are thus proportional to $(\Lambda_c - \Lambda)^{1/2}$ for $\Lambda \lesssim \Lambda_c$.

Inserting Eq. (78) into the flow equation (62) for m_σ^2 and neglecting the last fluctuation term, which is of higher order in α , one obtains

$$\partial_\Lambda m_\sigma^2 = -4I - \lambda \int_{q|\Lambda_b} [3G_\sigma(q) + G_\pi(q)]. \quad (79)$$

This shows that the flow of α and m_σ^2 is indeed consistent with the relation $m_\sigma^2 = \lambda\alpha^2$ following from the ansatz for the bosonic potential.

B. Infrared asymptotics

In the infrared limit ($\Lambda \rightarrow 0$) the key properties of the flow can be extracted from the flow equations analytically. The behavior of the bosonic sector depends strongly on the dimensionality of the system. We consider dimensions $d \geq 2$, focusing in particular on the two- and three-dimensional case.

The bosonic order parameter and the fermionic gap saturate at finite values in the limit $\Lambda \rightarrow 0$. The fluctuation corrections to $\partial_\Lambda \alpha$ and $\partial_\Lambda \Delta$ involve the singular Goldstone propagator G_π only linearly and are therefore integrable in $d > 1$. The fermion-boson interactions g_σ and g_π also saturate. The finiteness of Z_π and A_π is guaranteed by Ward identities.²³ In our truncation Z_π and A_π remain finite since only fermionic fluctuations contribute to the Goldstone propagator. We choose

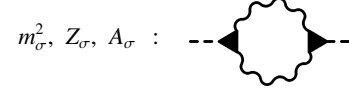


FIG. 8: Goldstone fluctuations determining the infrared asymptotics for $\Lambda \rightarrow 0$.

$\Lambda_b = \Lambda$ in the following. The choice of Λ_f (as a function of Λ) will be discussed and specified below.

The flows of m_σ^2 , λ , Z_σ , and A_σ are dominated by terms quadratic in G_π for $\Lambda \rightarrow 0$, see Fig. 8. Using $m_\sigma^2 = \lambda\alpha^2$, we obtain the asymptotic flow equation for λ from Eq. (62) in the simple form

$$\partial_\Lambda \lambda = \lambda^2 \int_{q|\Lambda} G_\pi^2(q). \quad (80)$$

The above integral over G_π^2 is proportional to Λ^{d-4} for small Λ in dimensions $d < 4$, implying that λ scales to zero in $d \leq 3$. In two dimensions one obtains $\int_{q|\Lambda} G_\pi^2(q) = \frac{1}{4\pi^2 A_\pi Z_\pi} \Lambda^{-2}$ for small Λ , such that the rescaled variable $\tilde{\lambda} = \lambda/\Lambda$ obeys the flow equation

$$\frac{d\tilde{\lambda}}{d \log \Lambda} = -\tilde{\lambda} + \frac{\tilde{\lambda}^2}{4\pi^2 A_\pi Z_\pi}, \quad (81)$$

which has a stable fixed point at $\tilde{\lambda}^* = 4\pi^2 A_\pi Z_\pi$. Hence, the bosonic self-interaction vanishes as

$$\lambda \rightarrow 4\pi^2 A_\pi Z_\pi \Lambda \quad \text{for } \Lambda \rightarrow 0 \quad (82)$$

in two dimensions. Consequently, also the radial mass m_σ^2 of the Bose fields vanishes linearly in Λ . In three dimensions one has $\int_{q|\Lambda} G_\pi^2(q) \propto \Lambda^{-1}$ for small Λ such that λ and m_σ^2 scale to zero logarithmically for $\Lambda \rightarrow 0$. Since m_σ^2 is the dominant contribution to the denominator of G_σ at small momenta and frequencies, the scaling of m_σ^2 to zero as a function of Λ implies that G_σ (at $\Lambda = 0$) diverges as

$$G_\sigma(sq) \propto s^{-1} \quad \text{for } d = 2 \quad (83)$$

$$G_\sigma(sq) \propto \log s \quad \text{for } d = 3 \quad (84)$$

in the limit $s \rightarrow 0$. Although derived from an approximate truncation of the functional flow equation, this result is *exact* even in two dimensions, where the renormalization of m_σ^2 is very strong. This is due to the fact that the scaling dimension of m_σ^2 is fully determined by the scaling dimension of the Goldstone propagator and the existence of a fixed point for $\tilde{\lambda}$, but does not depend on the position of the fixed point.²³

The flow of Z_σ is given by

$$\partial_\Lambda Z_\sigma = \frac{(\lambda\alpha)^2}{2} \int_{q|\Lambda} \partial_{p_0}^2 G_\pi(p+q) G_\pi(q) \Big|_{p=0} \quad (85)$$

for small Λ . The integral over the second derivative of $G_\pi G_\pi$ is of order Λ^{d-6} . In two dimensions the coupling λ vanishes

linearly in Λ , such that $\partial_\Lambda Z_\sigma \propto \Lambda^{-2}$, implying that Z_σ diverges as Λ^{-1} for $\Lambda \rightarrow 0$. Hence, the term $Z_\sigma q_0^2$ with $|q_0| = \Lambda$ in the denominator of G_σ scales linearly in Λ , as m_σ^2 . In three dimensions $\int_{|q|<\Lambda} \partial_{p_0}^2 G_\pi(p+q)G_\pi(q)|_{p=0}$ diverges as Λ^{-3} , while λ vanishes only logarithmically. Hence $\partial_\Lambda Z_\sigma \propto (\log \Lambda)^{-2} \Lambda^{-3}$, which is larger than in two dimensions. Integrating over Λ one finds $Z_\sigma \propto (\Lambda \log \Lambda)^{-2}$, which means that $Z_\sigma q_0^2$ vanishes as $(\log \Lambda)^{-2}$ in the infrared limit. This yields a subleading logarithmic correction to the mass term m_σ^2 in the denominator of G_σ . An analogous analysis with the same results as just obtained for Z_σ also holds for the momentum renormalization factor A_σ . A strong renormalization of longitudinal correlation functions due to Goldstone fluctuations appears in various physical contexts.^{30,31} Recently, a singular effect of Goldstone fluctuations on the fermionic excitations in a superfluid was found in Gaussian approximation.³² This singularity appears only after analytic continuation to real frequencies, and its fate beyond Gaussian approximation remains to be clarified.

Since m_σ^2 and λ scale to zero in the infrared limit in $d \leq 3$, all purely bosonic contributions to the effective action scale to zero. On the other hand, the fermion-boson coupling remains finite. One is thus running into a strong coupling problem, indicating a failure of our truncation, if fermionic fields are integrated too slowly, compared to the bosons. The problem manifests itself particularly strikingly in the flow equation for the order parameter, Eq. (60), in two dimensions. Since $m_\sigma^2 \propto \Lambda_b$ for small Λ_b , the fermionic contribution to $\partial_\Lambda \alpha$ is of order Λ^{-1} if one chooses $\Lambda_f = \Lambda_b = \Lambda$, leading to a spurious divergence of α for $\Lambda \rightarrow 0$.

The problem can be easily avoided by integrating the fermions fast enough, choosing $\Lambda_f \ll \Lambda_b$ in the infrared limit. In our numerical solution of the flow equations in the following section we will choose $\Lambda_b = \Lambda$ and $\Lambda_f = \Lambda^2/\Lambda_c$ for $\Lambda < \Lambda_c$, which matches continuously with the equal choice of cutoffs for $\Lambda > \Lambda_c$. The fermionic contribution to $\partial_\Lambda \alpha$ in Eq. (60) is then finite for small Λ , since the factor $\Lambda_f' = 2\Lambda$ in $\int_{|k|<\Lambda_f}$ compensates the divergence of m_σ^{-2} in front of the integral. Since the fermions are gapped below Λ_c , one could also integrate them completely (set Λ_f to zero), and then compute the flow driven by Λ_b only. The freedom to choose fermionic and bosonic cutoffs independently was exploited also in a recent fRG-based computation of the fermion-dimer scattering amplitude in vacuum.³⁴

C. Numerical results in two dimensions

In this section, we present a numerical solution of our flow equations from Sec. IVC in two dimensions. Technically, we employ a fifth-order Runge-Kutta integration routine²⁸ to solve coupled, ordinary differential equations. At each increment of the Runge-Kutta routine, two-dimensional integrations over the whole Brillouin zone have to be executed. For this purpose, we employ an integrator for singular functions²⁸ with relative error of less than 1%. In particular, for $\Lambda \approx \Lambda_c$ it is imperative to operate with sufficiently accurate routines as the integrands are large and small deviations result in a signif-

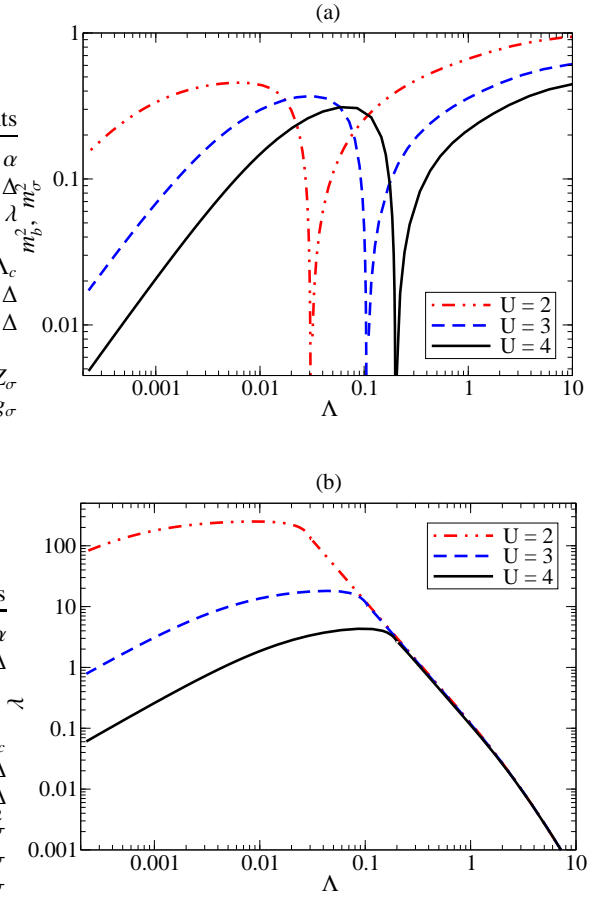


FIG. 9: (color online) (a): Flows of the bosonic mass, m_b^2 for $\Lambda > \Lambda_c$ and m_σ^2 for $\Lambda < \Lambda_c$. (b): Quartic coupling λ .

icant spread in the final values for $\Lambda \rightarrow 0$.

We fix our energy units by setting the hopping amplitude $t = 1$. We choose a chemical potential $\mu = -1.44$ corresponding to an average electron density of $1/2$ (quarter-filled band). This choice represents the generic case of a convex Fermi surface remote from van Hove singularities. The only varying input parameter is the Hubbard U , which determines the initial value of the bosonic mass via $m_b^2 = |2/U|$.

Initially, the flow starts in the symmetric regime with $\Lambda = \Lambda_0 = 100$, where Eqs. (55 - 58) determine the evolution. The critical scale is determined by the condition $m_b^2(\Lambda_c) = 0$. In the symmetry-broken regime ($\Lambda < \Lambda_c$), Eqs. (60 - 66) determine the evolution.

In Fig. 9 characteristic flows of the bosonic mass and the quartic coupling are shown in double-logarithmic plots for different choices of the Hubbard U . The sharp de- and increase of the bosonic mass marks the region around Λ_c . For small Λ , the flow reaches the infrared asymptotic regime (see Sec. VB). The scale Λ_{IR} at which this scaling sets in decreases for decreasing U . The numerically obtained scaling $m_\sigma^2, \lambda \propto \Lambda$ is consistent with the analytical result of Sec. VB.

In Fig. 10 (a) we compare the fermion gap with the bosonic order parameter (final values at $\Lambda = 0$) and the critical scale as

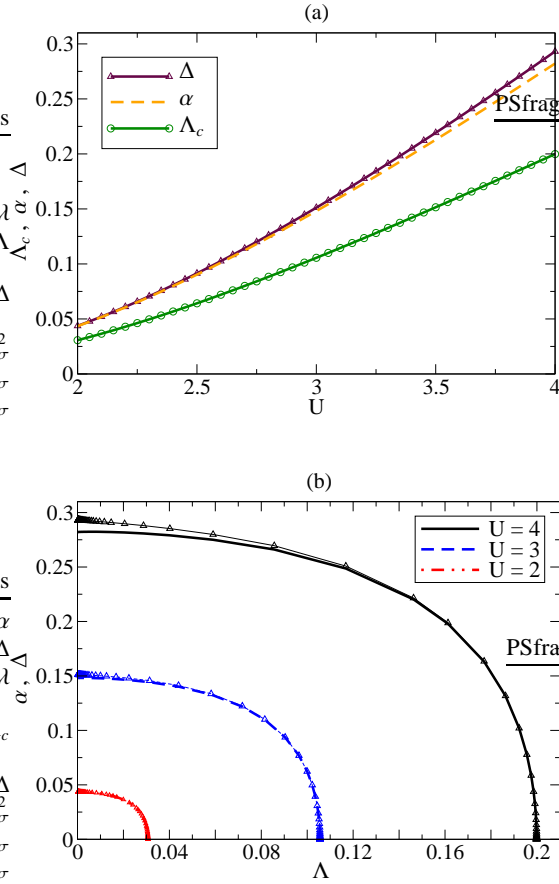


FIG. 10: (color online) (a): Fermion gap Δ , order parameter α , and the critical scale Λ_c versus Hubbard U . (b): Exemplary flows for Δ (triangles) and α (lines) each corresponding to one point in (a).

a function of U . In Fig. 10 (b) the flow of Δ and α as a function of Λ is shown for various choices of U . We observe $\Delta, \alpha \propto (\Lambda_c - \Lambda)^{1/2}$ for $\Lambda \lesssim \Lambda_c$ as derived below Eq. (78). The ratio Δ/Λ_c , where Δ is the final gap for $\Lambda \rightarrow 0$, is approximately 1.4 for the values of U studied here. As a result of fluctuations, the gap is reduced considerably compared to the mean-field result

$$\frac{\Delta}{\Delta_{\text{BCS}}} \approx 0.25 \quad (86)$$

for $2 \leq U \leq 4$. The main reduction here stems from the bosonic self-interactions in the symmetric regime leading to a substantial decrease of Λ_c via the second term of Eq. (55). A reduction of the gap compared to the mean-field value is generally present even in the weak coupling limit $U \rightarrow 0$. In fermionic perturbation theory second order corrections reduce the prefactor of the BCS gap formula even for $U \rightarrow 0$.³³ The reduction obtained here is slightly stronger than what is expected from a fermionic renormalization group calculation.⁷

For $\Lambda < \Lambda_c$, Goldstone fluctuations slightly reduce α via the term involving $G_\pi(q)$ in Eq. (60). On the other hand, the term due to the Goldstone mode in Eq. (61) enhances the fermionic gap Δ relative to α , such that Δ is generally slightly

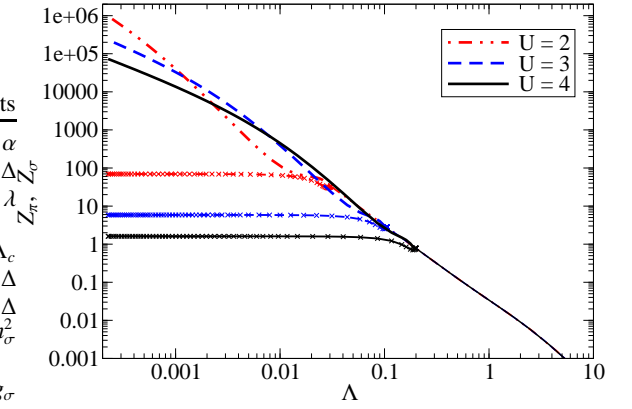


FIG. 11: (color online) Flows of Z_σ (lines) and Z_π (crosses).

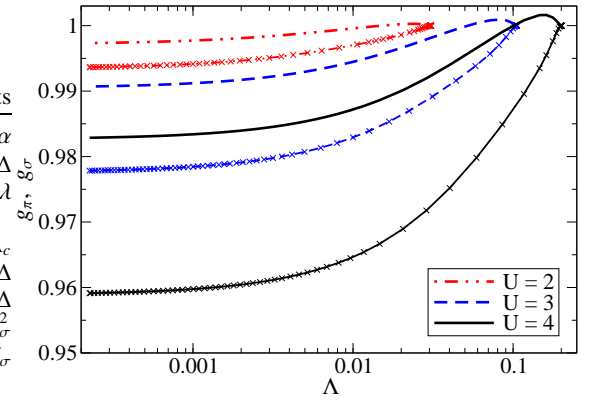


FIG. 12: (color online) Flows of fermion-boson vertices, g_σ (lines), and g_π (lines with crosses), for $\Lambda < \Lambda_c$.

larger than α . This difference will become larger upon increasing the interaction strength as one enters the regime of a Bose gas made of tightly bound fermions. Here, however, for relatively weak interactions, the impact of Goldstone fluctuations on both α and Δ is very modest. By contrast, the impact of Goldstone fluctuations is known to be dramatic at finite temperatures (not treated here) in two dimensions, since they drive the order parameter to zero.²⁹

In Fig. 11, we show flows of the Z-factors of the σ - and π -field, respectively. In the symmetric regime, the evolution is independent of U . At Λ_c , the ϕ -field splits into the σ - and π -modes with Z_σ diverging in the limit $\Lambda \rightarrow 0$ as $Z_\sigma \propto \Lambda^{-1}$ (cf. Sec. VB). The Z-factor of the Goldstone field saturates for $\Lambda \ll \Delta$. The flows for the A-factors (not shown) parametrizing the momentum dependence of the σ - and π -propagators exhibit very similar behavior.

Finally, in Fig. 12 we show flows of the fermion-boson vertices g_σ and g_π for $\Lambda < \Lambda_c$. Their relative changes are only of the order of a few percent (note the scale of the vertical axis) with g_σ being a bit larger than g_π .

VI. CONCLUSION

Truncating the exact fRG flow, we have derived approximate flow equations which capture the non-trivial order parameter fluctuations in the superfluid ground state of the attractive Hubbard model, which has been chosen as a prototype model for attractively interacting fermions. The superfluid order parameter is associated with a bosonic field which is introduced via a Hubbard-Stratonovich decoupling of the fermionic interaction. Below a critical scale Λ_c , the bosonic effective potential assumes a mexican hat shape leading to spontaneous symmetry breaking and a Goldstone mode. The bosonic order parameter is linked to but not equivalent to a fermionic gap. The fermionic gap is significantly smaller than the mean-field gap, mostly due to fluctuations above the scale Λ_c . Transverse order parameter fluctuations (Goldstone mode) below Λ_c lead to a strong renormalization of radial fluctuations. The radial mass and the bosonic self-interaction vanish linearly as a function of the scale in two dimensions, and logarithmically in three dimensions, in agreement with the exact behavior of an interacting Bose gas.²³ On the other hand, the average order parameter, the fermionic gap, and the interaction between fermions and bosons are affected only

very weakly by the Goldstone mode.

Supplementing the flow equations derived above by a shift of the chemical potential, to keep the density fixed, one may also try to deal with larger values of U . Eagles³⁵ and Leggett³⁶ have shown that already the BCS mean-field theory captures many features of the condensed Bose gas ground state made from strongly bound fermion pairs in the limit of strong attraction. Beyond mean-field theory, the difference between the fermionic gap and the order parameter α increases at larger U . It will also be interesting to extend the present analysis to $T > 0$, in particular in view of the possibility of a finite fermionic gap in the absence of long-range order in a Kosterlitz-Thouless phase at low finite temperatures.

Acknowledgments

We thank S. Diehl, S. Floerchinger, H. Gies, P. Jakubczyk, A. Katanin, H. C. Krahl, P. Kopietz, J. Pawłowski, M. Salmhofer, M. Scherer, and R. Zeyher for very useful discussions. S. Diehl and P. Jakubczyk are gratefully acknowledged for critically reading the manuscript.

-
- * Electronic address: p.strack@fkf.mpg.de
- ¹ For a review, see J. Berges, N. Tetradis, and C. Wetterich, Phys. Rep. **363**, 223 (2002).
 - ² For a short review of the fRG applied to Fermi systems, see W. Metzner, Prog. Theor. Phys. Suppl. **160**, 58 (2005).
 - ³ M. Salmhofer, C. Honerkamp, W. Metzner, and O. Lauscher, Prog. Theor. Phys. **112**, 943 (2004).
 - ⁴ R. Gersch, J. Reiss, and C. Honerkamp, New J. Phys. **8**, 320 (2006).
 - ⁵ A.A. Katanin, Phys. Rev. B **70**, 115109 (2004).
 - ⁶ R. Gersch, C. Honerkamp, D. Rohe, and W. Metzner, Eur. Phys. J. B **48**, 349 (2005).
 - ⁷ R. Gersch, C. Honerkamp, and W. Metzner, arXiv:0710.0238.
 - ⁸ T. Baier, E. Bick, and C. Wetterich, Phys. Rev. B **70**, 125111 (2004).
 - ⁹ F. Schütz, L. Bartosch, and P. Kopietz, Phys. Rev. B **72**, 035107 (2005).
 - ¹⁰ F. Schütz and P. Kopietz, J. Phys. A **39**, 8205 (2006).
 - ¹¹ B. Krippa, Eur. Phys. J. A **31**, 734 (2007).
 - ¹² H. C. Krahl, and C. Wetterich, Phys. Lett. A **367**, 263 (2007).
 - ¹³ S. Diehl, H. Gies, J. M. Pawłowski, and C. Wetterich, Phys. Rev. A **76**, 021602(R) (2007).
 - ¹⁴ For a review of the attractive Hubbard model (and extensions) see R. Micnas, J. Ranninger, and S. Robaszkiewicz, Rev. Mod. Phys. **62**, 113 (1990).
 - ¹⁵ For a review, see M. Randeria, in *Bose-Einstein Condensation*, edited by A. Griffin, D. Snoke, and S. Stringari (Cambridge University Press, Cambridge, England, 1995), pp. 355-392.
 - ¹⁶ M. Keller, W. Metzner, and U. Schollwöck, Phys. Rev. Lett. **86**, 4612 (2001).
 - ¹⁷ W. Hofstetter, J. I. Cirac, P. Zoller, E. Demler, and M. D. Lukin, Phys. Rev. Lett. **89**, 220407 (2002).
 - ¹⁸ D. Jaksch, and P. Zoller, Ann. Phys. **315**, 52 (2005).
 - ¹⁹ J. K. Chin, D. E. Miller, Y. Liu, C. Stan, W. Setiawan, C. Sanner, K. Xu, and W. Ketterle, Nature **446**, 961 (2006).
 - ²⁰ R. B. Diener, R. Sensarma, and M. Randeria, Phys. Rev. A **77**, 023626 (2008).
 - ²¹ J. Feldman, J. Magnen, V. Rivasseau, and E. Trubowitz, Helv. Phys. Acta **66**, 497 (1993).
 - ²² Y.A. Nepomnashchy, Phys. Rev. B **46**, 6611 (1992), and references therein.
 - ²³ F. Pistolesi, C. Castellani, C. Di Castro, and G.C. Strinati, Phys. Rev. B **69**, 024513 (2004); Phys. Rev. Lett. **78**, 1612 (1997).
 - ²⁴ V.N. Popov, *Functional integrals and collective excitations* (Cambridge University Press, Cambridge, 1987).
 - ²⁵ J.W. Negele and H. Orland, *Quantum Many-Particle Systems* (Addison-Wesley, Reading, MA, 1987).
 - ²⁶ C. Wetterich, Phys. Lett. B **301**, 90 (1993).
 - ²⁷ For a comprehensive discussion of the Goldstone mode in the context of critical behavior see, C. Wetterich, Z. Phys. C **57**, 451 (1991).
 - ²⁸ GSL-GNU scientific library, <http://www.gnu.org/software/gsl/>.
 - ²⁹ N. Goldenfeld, *Lectures on Phase Transitions and the Renormalization Group* (Perseus Publishing, Oxford, 1992).
 - ³⁰ P. B. Weichman, Phys. Rev. B **38**, 8739 (1988).
 - ³¹ W. Zwerger, Phys. Rev. Lett. **92**, 027203 (2004).
 - ³² N. Lerch, L. Bartosch, and P. Kopietz, Phys. Rev. Lett. **100**, 050403 (2008).
 - ³³ A. Martín-Rodero and F. Flores, Phys. Rev. B **45**, 13008 (1992).
 - ³⁴ S. Diehl, H. C. Krahl, and M. Scherer, arXiv:0712.2864.
 - ³⁵ D. M. Eagles, Phys. Rev. **186**, 456 (1969).
 - ³⁶ A. J. Leggett, in *Modern Trends in the Theory of Condensed Matter*, edited by A. Pekalski and R. Przystawa (Springer, Berlin, 1980).